INSTITUTE OF PHYSICS PUBLISHING JOURNAL OF PHYSICS: CONDENSED MATTER

J. Phys.: Condens. Matter **16** (2004) 5979–5990 PII: S0953-8984(04)79143-2

Crystalline structure and the superconducting properties of NbB_{2+x}

R Escamilla[1], O Lovera[1], T Akachi[1], A Durán[2], R Falconi[1], F Morales[1] and R Escudero[1]

[1] Instituto de Investigaciones en Materiales, Universidad Nacional Autónoma de México, Apartado Postal 70-360, México DF, 04510, Mexico
[2] Centro de Ciencias de la Materia Condensada, Universidad Nacional Autónoma de México, Apartado Postal 2681, Ensenada BC, 22800, Mexico

Received 13 April 2004
Published 30 July 2004
Online at stacks.iop.org/JPhysCM/16/5979
doi:10.1088/0953-8984/16/32/029

Abstract

The effect of boron excess in the structure and superconducting properties of NbB_2 is reported. Rietveld refinements of the x-ray diffraction patterns indicate that boron excess induces significant changes in the Nb–B bond length, increasing the *c*-axis. In contrast, the B–B bond length remains essentially constant. Magnetization behaviour was studied in the temperature range from 2 to 15 K. We found that for $(B/Nb)_{exp} \geqslant 2.20(2)$ of boron excess samples display superconductivity with a maximum T_C of about 9.8 K at $(B/Nb)_{exp} = 2.34(1)$. High pressure measurements in samples with two different boron contents reveal that T_C decreases at different ratios, dT_C/dP. Superconducting parameters were determined, indicating that NbB_{2+x} is a type II superconductor. We correlated the change of T_C with the evolution of the structural parameters and found that it coincides with theoretical predictions of band structure.

(Some figures in this article are in colour only in the electronic version)

1. Introduction

The discovery of superconductivity in MgB_2 at about 40 K by Nagamatsu *et al* [1] has generated a great deal of excitement, and many studies related to fundamental and practical aspects of the material have been performed. Much research has investigated other diborides expecting to find higher transition temperatures, but without success. NbB_2 is a diboride which has been studied recently; this compound is interesting because of its similar behaviour to MgB_2. This fact has conduced us to study the superconducting and crystallographic characteristics when B excess is introduced; in this work we will analyse its general behaviour.

Before describing details of the compound under study, such as the crystalline and superconducting characteristics of $Nb_{1+x}B_2$, it will be necessary to introduce details of MgB_2 related to defects in the structure, and their influence on the superconducting properties. Actually this is a matter of debate, due to the inherent difficulties in synthesis and to the exact details of the crystalline structure. The stoichiometry of this compound can slightly be modified [2], mainly due to the high ionicity of the Mg–B bond. Theoretical studies related to band structure [3] clearly reveal that while the B–B bond is covalent the Mg–B bond is highly ionic [4]. From the experimental and theoretical points of view, it is known that the high transition temperature in MgB_2 is essentially related to the large value of the electron–phonon coupling constant, λ, and to the participation of the high phonon frequency: the E_{2g} vibrational mode.

Earlier experiments showed that for other MB_2 diborides (M = Ti, Zr, Hf, V, Nb, Ta, Cr, Mo) T_C is below 0.4 K [5]. Nevertheless, only NbB_2 has shown moderate superconducting transition temperature depending on the preparation route [6–12]. Studies for stoichiometric NbB_2 reveal a T_C of about 5.2 K [13], whereas other studies reported the absence of superconductivity down to 2 K [5]. However, metal-deficient $Nb_{1-x}B_2$ has shown a transition temperature at about 9.2 K when it was prepared under high pressure conditions [12]. Also it has been found by Schirber *et al* [10] that a NbB_x single crystal with x near 2 shows a maximum $T_C = 9.4$ K, when measured under high pressure conditions of about 5 kbar.

Theoretical studies related to band structure of NbB_2 by Shein and Ivanovskii [3] show an enhancement of the covalent interactions between boron and Nb planes (due to hybridization of the B 2p–Nb d states), which in turn changes the density of states at the Fermi level $N(E_F)$; this fact must also be valid for the non-stoichiometric NbB_{2+x} compound. Then, $N(E_F)$ will change with the atomic ratio B/Nb, giving a peak in the density of states at the Fermi level, T_C thus reaching a maximum value [3]. In this context it will be interesting to probe theoretical predictions by performing systematic experimental studies in non-stoichiometric NbB_2, in order to understand the role of excess boron in structural and superconducting properties of the compound. In this work we will show the importance of defects in the electronic properties of NbB_2.

We report that in NbB_{2+x}, careful synthesizing procedures allow us to increase the transition temperature to about 9.8 K, for $(B/Nb)_{exp}$ in the range 2.32(1)–2.34(1). We analyse the changes of the lattice parameters due to boron excess, and the superconducting state. Additionally we compared this behaviour with our high pressure experiments performed using a diamond anvil cell.

2. Experimental details

NbB_{2+x} samples were prepared at different boron contents, from B/Nb = 2.0 to 2.6, by solid-state reaction (B/Nb means the starting B excess in the sintering reaction). Precursors from Aldrich were NbB_2, 325 mesh, and boron 99.5% $<$ 60 mesh. Both were mixed and pressed into pellets with different compositions, placed in sealed stainless steel tubes under Ar atmosphere, and sintered in a tube furnace at 1000 °C; after 3 h they were quenched to room temperature. The process was repeated after grinding the sintered material. Phase identification was performed with an x-ray diffractometer (XRD) Siemens D5000 using Cu Kα radiation and a Ni filter. Intensities were measured in small steps of 0.02°, from 10° to 120° at room temperature. Crystallographic parameters were refined with the program Quanto (Rietveld program for quantitative phase analysis of polycrystalline samples) [14].

Magnetization measurements were performed in a SQUID based magnetometer (Quantum Design) at zero field cooling (ZFC) and field cooling (FC) conditions, under 5 Oe magnetic field. Resistance versus temperature (R–T) measurements were performed at different

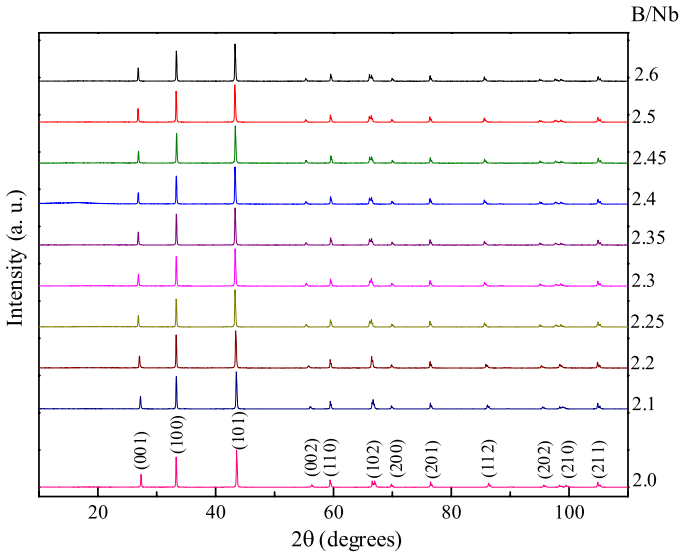

Figure 1. X-ray diffraction patterns of the NbB_{2+x} for $2.0 \leqslant B/Nb \leqslant 2.6$ of nominal composition.

pressures. Powder samples were mechanically compacted and shaped to appropriate sizes and mounted into a diamond anvil cell (DAC) with diamonds of 500 μm culet size. Cu–Be gaskets were used to perform the quasi-hydrostatic measurements; they were filled with fine powder of MgO < 2 μm size. Four gold wires of 10 μm diameter were used for the R–T measurements. The experiments were performed from room temperature to about 1.6 K. The pressure calibration was determined with the change of the superconducting temperature of Pb. Additional information about high pressure measurements and procedures can be found in Falconi *et al* [15].

3. Results and discussion

Figure 1 shows the powder x-ray diffraction patterns of NbB_{2+x} samples with nominal compositions B/Nb from 2.0 to 2.6. These correspond to the NbB_2 common structure (No 75-1048 of the International Centre for Diffraction Data ICDD). The impurities observed are faint features of Nb_5B_6 (ICDD No 42-1040), B_2O_3 (ICDD No 76-1655) and Nb_2O_5 (ICDD No 80-2493). Diffraction patterns were fitted using Rietveld analysis, with the hexagonal AlB_2 structure model and space group $P6/mmm$ (No 191). The analysis shows that the majority phase is $NbB_{2+x} > 90\%$. Figure 2 shows an example of the Rietveld analysis for the composition with B/Nb = 2.0.

Structural analysis extracted from Rietveld refining considering NbB_{2+x} structure, see figure 3, indicates the occupancy factor for niobium and boron as a function of boron excess. However, the real niobium occupation factor is included in table 1 using the $Nb_{1-x}B_2$ stoichiometry. This must be compared to the boron nominal starting compositions, B/Nb. It seems that for compositions below $B/Nb \leqslant 2.3$ both are similar. As the nominal composition increases from B/Nb = 2.35 to 2.6 Rietveld refining determines the real composition, given $(B/Nb)_{exp} = 2.30(1)$–$2.34(2)$ with respect to the B/Nb values. The structural parameter data are listed in table 1. Figure 4 shows the evolution of the lattice parameters and cell

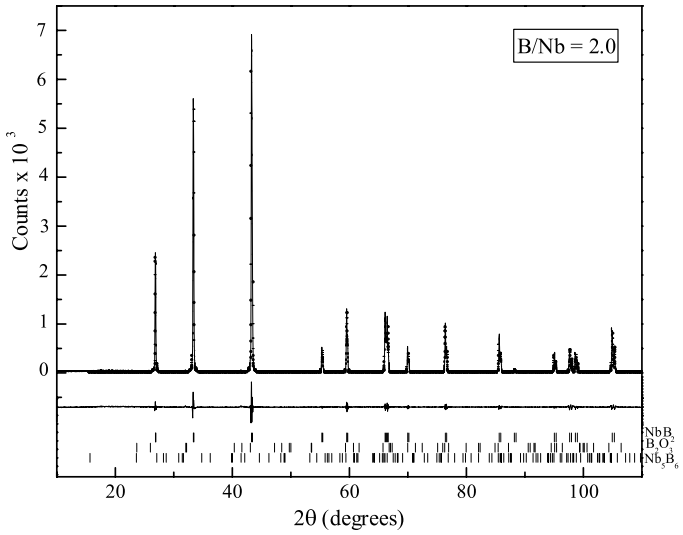

Figure 2. Example of Rietveld refinement for the NbB_2 sample. X-ray experimental diagram (dots), and calculated pattern (continuous curve), difference (middle curve) and calculated peak positions (bottom).

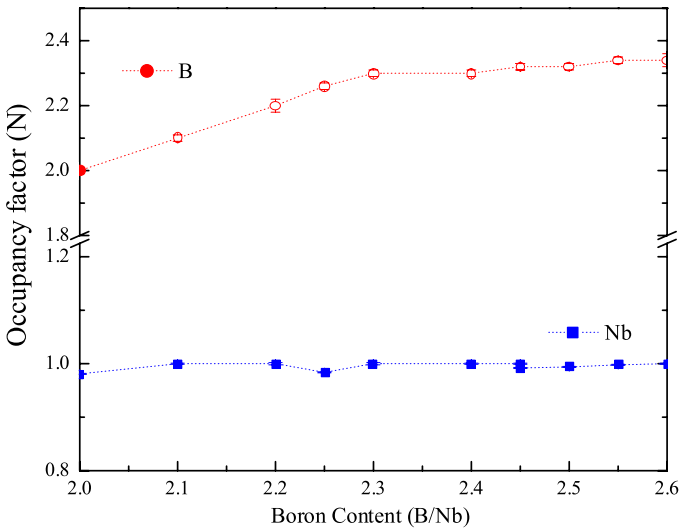

Figure 3. Occupancy factor for Nb and B metals in NbB_{2+x} as determined by Rietveld analysis.

volume as a function of boron content at room temperature. We observed that the a-axis decreases slightly as $(B/Nb)_{exp}$ increases, while the c-axis increases continuously in the interval $2.00(1) \leqslant (B/Nb)_{exp} \leqslant 2.26(1)$, and remains almost constant from about $B/Nb = 2.3$ to 2.6. As a consequence of these changes the unit cell volume increases in the composition interval $2.00(1) \leqslant (B/Nb)_{exp} \leqslant 2.26(1)$ and remains almost constant in the interval $2.30(1) \leqslant (B/Nb)_{exp} \leqslant 2.34(2)$.

Similar results have been observed in other studies related to high pressure synthesis in the hole-doped Nb_xB_2, [12]. The authors observed that when x is increased, the a-axis decreases,

Table 1. Structural parameters for NbB_{2+x} at 295 K. Space group: $P6/mmm$ (No 191). Atomic positions: Nb, 1a (0, 0, 0); B, 2d (1/3, 2/3, 1/2). (Note: space group is $P6/mmm$ (No 191) and the atomic positions are as follows: Nb, 1a (0, 0, 0); B, 2d(1/3, 2/3, 1/2), B/Nb—nominal boron to metal ratio; B/Nb_{exp}—experimentally determined boron to metal ratio in sample. B in $Å^2$ and N are the isotropic thermal and occupancy parameters. Numbers in parentheses are the estimated standard deviation of the last significant digit.)

B/Nb	2.0	2.1	2.2	2.25	2.3	2.35	2.4	2.45	2.5	2.55	2.6
a (Å)	3.110(2)	3.110(2)	3.108(3)	3.104(2)	3.105(2)	3.104(2)	3.104(2)	3.104(2)	3.104(2)	3.104(2)	3.104(2)
c (Å)	3.267(2)	3.282(3)	3.296(3)	3.317(3)	3.316(3)	3.319(2)	3.319(3)	3.320(2)	3.319(3)	3.321(2)	3.320(3)
V ($Å^3$)	27.369	27.488	27.578	27.677	27.683	27.696	27.695	27.704	27.690	27.699	27.701
c/a	1.050	1.055	1.060	1.068	1.068	1.069	1.070	1.070	1.069	1.070	1.070
B/Nb_{exp}	2.00(1)	2.10(1)	2.20(2)	2.26(1)	2.30(1)	2.30(1)	2.32(1)	2.32(1)	2.34(1)	2.34(1)	2.34(2)
$N_{(Nb)}$	0.986(1)	0.943(2)	0.909(1)	0.878(1)	0.869(1)	0.864(1)	0.857(1)	0.854(1)	0.848(1)	0.849(1)	0.848(1)
B ($Å^2$)$_{(Nb)}$	0.37(1)	0.12(1)	0.15(1)	0.07(1)	0.13(1)	0.14(1)	0.07(1)	0.14(1)	0.16(1)	0.17(2)	0.13(1)
B ($Å^2$)$_{(B)}$	0.8(1)	0.9(1)	0.9(2)	0.5(1)	1.4(1)	1.2(1)	1.0(1)	1.1(1)	1.6(1)	1.50(2)	1.38(1)
B–Nb bond length (Å)	2.426(3)	2.431(2)	2.435(3)	2.440(3)	2.441(2)	2.441(3)	2.441(3)	2.442(2)	2.441(3)	2.441(3)	2.441(2)
B–B bond length (Å)	1.794(2)	1.794(3)	1.793(2)	1.790(3)	1.791(2)	1.790(2)	1.790(3)	1.790(2)	1.790(3)	1.790(3)	1.790(2)
% NbB_{2+x}	95.23(2)	95.02(2)	96.13(2)	97.220(9)	95.40(2)	98.118(6)	97.910(8)	94.55(2)	98.219(6)	93.08(2)	94.36(2)
% Nb_5B_6	0.8(1)	1.31(8)	0.92(7)	0.80(8)	1.7(1)	0.23(4)-	0.36(5)	0.56(6)	0.24(3)	0.22(4)	0.69(8)
% B_2O_3	4.0(6)	3.5(4)	2.8(5)	1.9(3)	2.9(4)	1.3(2)	1.7(4)	4.8(5)	1.5(2)	6.7(5)	4.9(4)
% Nb_2O_5	—	0.18(7)	0.19(7)	—	—	0.33(7)	—	0.03(3)	0.08(6)	—	—
R_p (%)	12.1	11.5	13.4	11.7	12.2	11.2	10.0	10.6	11.4	9.8	10.9
R_{wp} (%)	17.3	16.7	18.7	16.4	17.3	16.2	13.8	15.8	16.7	14.5	16.4
Re (%)	12.3	12.4	12.6	12.7	12.5	12.1	11.0	12.5	12.4	11.7	12.5
GoF (%)	1.4	1.3	1.5	1.3	1.4	1.3	1.3	1.3	1.3	1.2	1.3

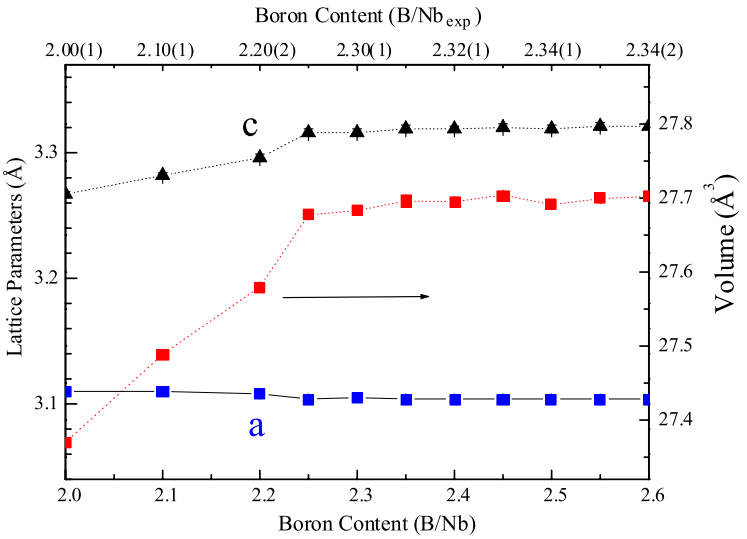

Figure 4. Crystal parameters and unit cell volume as a function of boron content ($(B/Nb)_{exp}$ or B/Nb).

whereas the *c*-axis is increased; this effect was attributed to Nb vacancies. Other studies with transition metal diborides show that boron excess is incorporated into the phase, creating vacancies in the metal site, rather than going into lattice interstitials [16]. The expectation that excess boron could be accommodated at interstitial sites comes from the closely related Mo_2B_{5-x} phase [17]. However, recent work [18] confirms the existence of a puckered plane, but does not locate the interstitial boron atoms. A subsequent study using neutron powder diffraction detected the interstitial boron sites, but with only a small occupancy [19]. So according to this evidence we are assuming in this study that the effect of boron excess is to create vacancies in Nb sites. Such a conclusion is in agreement with the fact that the honeycomb network of B is very rigid and therefore it will be very difficult to find interstitial spaces for additional B. Another indication related to structural characteristics is that when x is increased the B–B bond length associated to the basal plane decreases slightly, while the Nb–B bond length (along the *c*-axis) increases continuously in the $2.00(1) \leqslant (B/Nb)_{exp} \leqslant 2.26(1)$ range, remaining almost constant for $2.30(1) \leqslant (B/Nb)_{exp} \leqslant 2.34(2)$; this is shown in figure 5.

In order to corroborate the consequences of the increase of the *c*-axis length in the superconducting properties of this compound, it is worthwhile to study the effect of hydrostatic or quasi-hydrostatic high pressure (as also the equivalent effects) as well as the internal chemical pressure.

Slusky *et al* [20] investigated the substitution of Al on the Mg site, i.e. $(Mg_{1-x}Al_xB_2)$, and observed that T_C decreases smoothly with increasing x for $0 < x < 0.1$, accompanied by a slight decrease of the *c*-axis length. They concluded that the compound MgB_2 is near to a structural instability that can destroy superconductivity. On the other hand, high pressure diffraction studies at room temperature at several pressures from about 6 to 30 GPa [21–24] have been performed. These show that the *c*-axis length decreases faster with pressure than the *a*-axis length, demonstrating that the out-of-plane Mg–B bond is much weaker than the in-plane Mg–Mg bond. Accordingly, clearly the Mg–B bond length has an important influence in the superconducting behaviour of MgB_2. Going back to the structural characteristics and superconducting behaviour of NbB_{2+x} phase, this work shows that T_C increases as

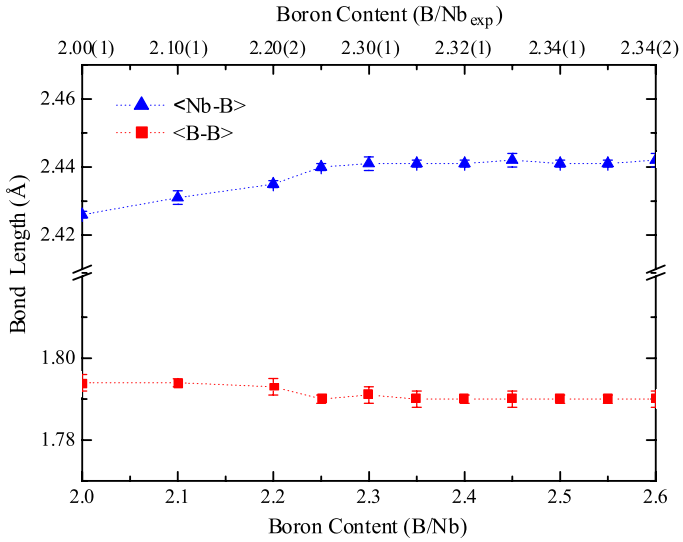

Figure 5. ⟨Nb–B⟩ and ⟨B–B⟩ bond lengths versus boron content.

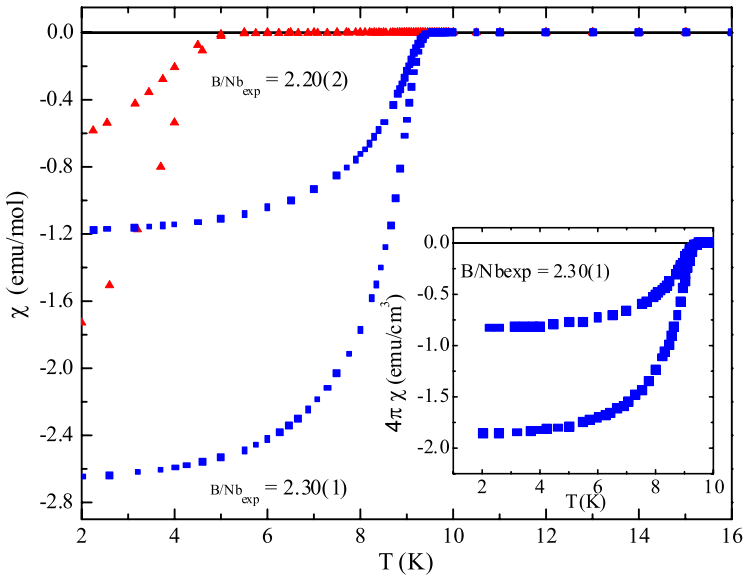

Figure 6. Susceptibility–temperature measurements showing the transition temperature (shielding and Meissner fraction) for two samples with different B concentrations. The inset shows the shielding and Meissner fractions in terms of $1/4\pi$.

boron excess is increased to the limit of about $(B/Nb)_{exp} = 2.34(1)$ where the transition temperature $T_C = 9.8$ K reaches a maximum. Figures 6 and 7 show results of magnetic measurements. The superconducting transition temperature, T_C, was defined at the onset of the diamagnetic response in $\chi(T)$. It must be pointed out that we did not detect superconductivity in $(B/Nb)_{exp} = 2.00(1)NbB_2$ and $(B/Nb)_{exp} = 2.10(1)NbB_{2.1}$. At compositions from $2.26(1) < (B/Nb)_{exp} < 2.34(2)$, the transition temperature increases continuously from

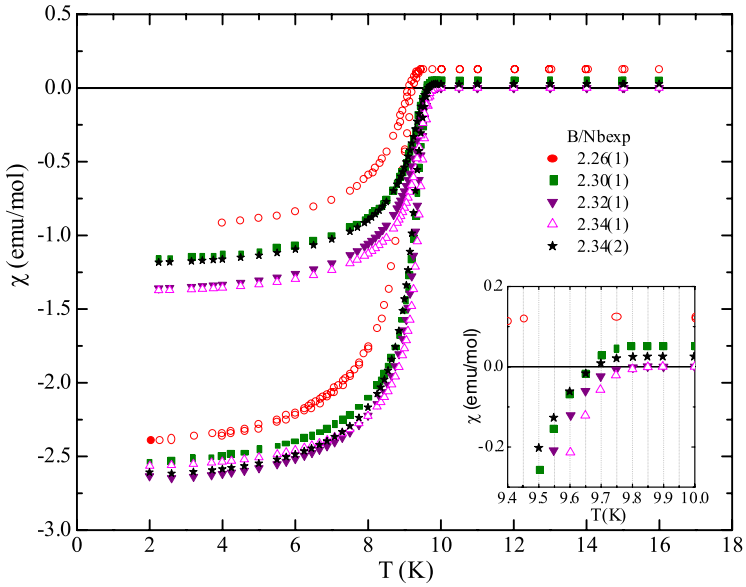

Figure 7. Temperature dependence of the susceptibility, from 2 to 15 K in applied magnetic field of 5 Oe for NbB_{2+x}, with different boron concentrations. The inset shows T_C decreasing for boron concentration higher than 2.32(1).

Table 2. Magnetic fields $H_{C1}(0)$ and $H_{C2}(0)$ estimated from experimental data at low temperature using a parabolic fit; $H_C(T) = H_C(0)[1 - (T/T_C)^2]$. Ginzburg–Landau parameters were determined from the GL equations.

T_C (K)	H_{C1} (Oe)	H_{C2} (Oe)	ξ_{GL} (nm)	κ_{GL}	λ_{GL} (nm)
9.75	196	2 226	40	2.49	87

5 K to a maximum of 9.8 K. In all these samples the Meissner fraction indicates bulk superconductivity. One example of the superconducting fraction can be seen in figure 6, where the Meissner and shielding fractions are plotted; the shielding fraction corresponds to about 190%. The estimated Meissner fraction was about 80%. Determination of the percentages used the theoretical density for $(B/Nb)_{exp} = 2.30(1)NbB_{2.3}$; see the inset of figure 6. In order to illustrate the T_C changes, the inset of figure 7 shows an amplification of the $\chi(T)$ curves around T_C values. For instance the composition with $(B/Nb)_{exp} = 2.26(1)$ shows a transition temperature at $T_C = 9.2$ K, and further increase of boron increases the transition temperature to 9.8 K. Above $(B/Nb)_{exp} = 2.34(1)$, T_C drops to about 9.4 K.

Following the characterization of the superconducting behaviour of this material, we used magnetization measurements as a function of applied magnetic field. We found that the compound behaves as a type II superconductor. Figure 8 shows the critical magnetic fields and table 2 shows the superconducting parameters. $H_{C1}(0)$ and $H_{C2}(0)$ were estimated from experimental data and a parabolic fit near zero temperature with the expression $H_C(T) = H_C(0)[1 - (T/T_C)^2]$ below 5 K. Ginzburg–Landau (GL) parameters such as coherence length ξ_{GL}, penetration length λ_{GL}, and κ were determined from the equations; $H_{C2}(0) = \Phi_0/2\pi\xi_{GL}^2$, $H_{C2}(0)/H_{C1}(0) = 2\kappa^2 \ln\kappa$, and $\lambda_{GL}^2 = \Phi_0 \ln\kappa/4\pi H_{C1}(0)$. In the equations $\Phi_0 = hc/2e \approx 2.07 \times 10^{-7}$ G cm^2 is the flux quantum. Thus, $\kappa = 2.49$ confirms that NbB_{2+x} is a type II superconductor.

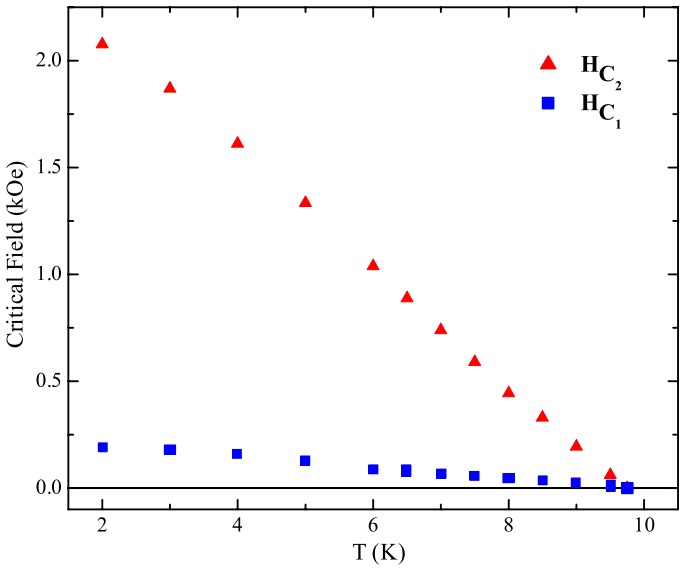

Figure 8. Critical fields H_{C1} and H_{C2} as functions of temperature for $(B/Nb)_{exp} = 2.32(1)$ determined from magnetic measurements.

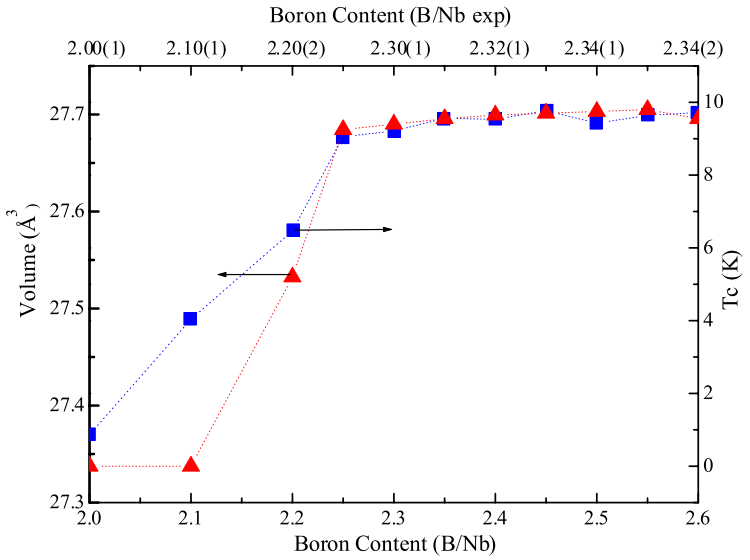

Figure 9. Cell volume and the superconducting transition T_C at different boron concentrations.

From the viewpoint of the chemical pressure effects, one important observation of this study is that T_C and cell volume increase in the same manner as boron content is increased. Figure 9 shows this behaviour. In order to see the external pressure effect on the superconducting characteristics we performed measurements at quasi-hydrostatic high pressure with diamond cells on two extreme compositions, $(B/Nb)_{exp} = 2.26(1)$, and 2.32(1). The corresponding R versus T curves at different pressures up to 5.9 GPa for the sample with composition $(B/Nb)_{exp} = 2.26(1)$ are shown in figure 10. The inset of this figure reveals in

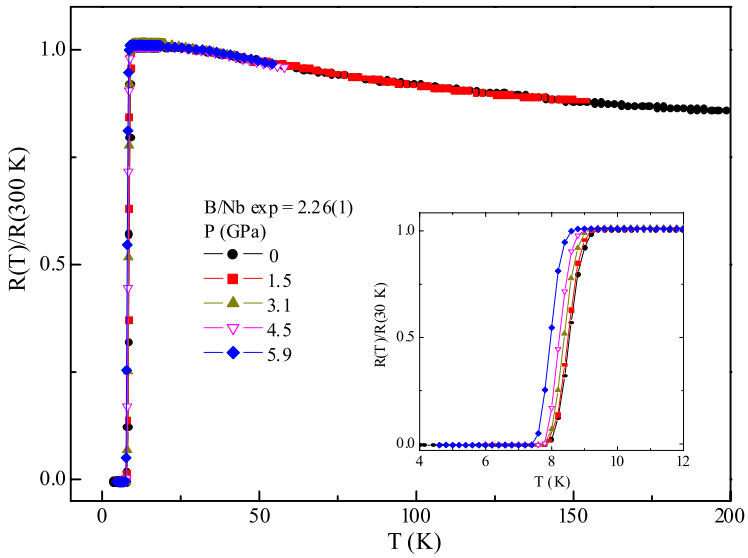

Figure 10. R versus T curves at different pressures up to 5.9 GPa for a sample with $(B/Nb)_{exp} = 2.26(1)$. The inset reveals details at low temperature.

detail the low temperature behaviour of curves and changes of the superconducting transition. Variation of T_C as function of temperature for the two compositions $(B/Nb)_{exp} = 2.26(1)$ and $(B/Nb)_{exp} = 2.32(1)$ (T_C determined as the 50% value of the resistance drops at the transition temperature) is shown in figure 11. As a matter for comparison, the inset shows the pressure variation of normalized T_C/T_{C0} (T_{C0} is the room pressure superconducting transition temperature). From those measurements we determined the ratios $dT_C/dP = -0.104$ and -0.054 K GPa^{-1} for samples with composition 2.26(1), and 2.32(1) respectively. It seems that the ratio of decreasing temperature with pressure is quite different for the two samples. First of all, it seems that the sample with higher boron content requires more pressure to decrease T_C, which implies a strong Nb–B bond, perhaps very close to the limit of strength. Secondly, the sample with $(B/Nb)_{exp} = 2.26(1)$ shows a higher value for dT_C/dP than the 2.32(1) composition; this suggests that the Nb–B bond presents less stiffness than the other composition with 2.32(1). The implication of these high pressure experiments is that we corroborate the hypothesis that reducing the bond length in the crystalline direction c (mainly) reduces T_C, via displacing the Fermi level to a minimum in $N(E)$; this in turn decreases the Coulombic repulsion and the alloy will be in a region with higher stability. Here we are invoking a mechanism of the Hume–Rothery type [25]. The reduction of T_C in our high pressure measurements is in clear contrast to the Schirber *et al* result, where they observe an increase of T_C under pressure to about 9.6 K, determined in a single crystal of NbB_x, with x close to 2.

Lastly, we explain the experimental results based on theoretical aspects. Band structure calculations [3] show that the band structure changes when boron content is increased; this in turn affects the density of states at the Fermi level, changing from a minimum to a maximum value. According to this, T_C must increase, following BCS theory. This fact was also explained for the decreasing T_C in the compound TaB_2, and the absence of superconductivity in VB_2 in terms of the considerable decrease in the contributions of the B 2p states to the density of states at the Fermi level. Such a B 2p contribution to $N(E_F)$ for the three compounds is

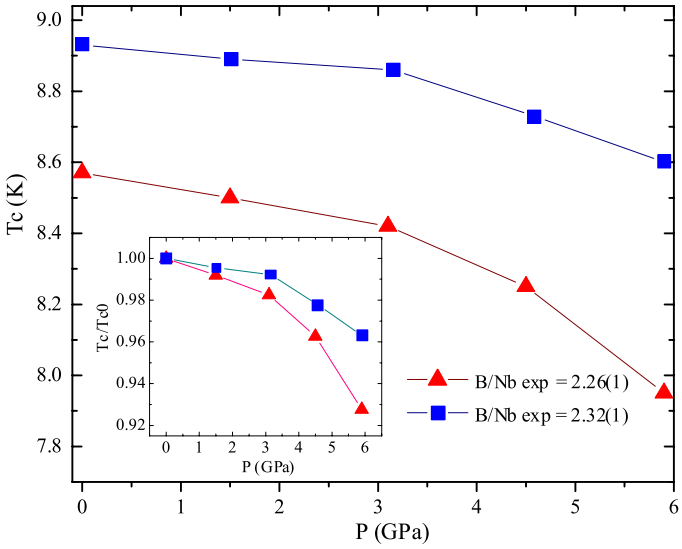

Figure 11. Pressure dependence of T_c for two compositions of NbB_{2+x}, with $(B/Nb)_{exp} = 2.26(1)$, and 2.32(1). The inset shows the normalized variation, T_C/T_{C0}, where T_{C0} is the superconducting transition temperature at room pressure.

$MgB_2(0.448)$, $TaB_2(0.178)$, and $VB_2(0.085)$ states eV^{-1}. We may conclude that on the basis of the previous ideas, and band calculations we can certainly assume that the increase in the excess boron generates an increase in the number of niobium vacancies (see table 1 [14]) which increases the number of carriers [12] by positioning the Fermi level at a maximum in $N(E)$.

4. Conclusions

In summary, we have reported studies on samples of NbB_{2+x} prepared by solid-state reaction at ambient pressure. Samples are superconducting with a maximum transition temperature at 9.8 K. XRD and Rietveld refinements show that boron excess induces significant changes in the Nb–B bond length, giving rise to an increase in the c-axis. The superconducting fraction determined in the samples was about 80%. The maximum T_C was obtained at boron concentrations in the range from $(B/Nb)_{exp} = 2.32(1)$ to 2.34(1). From structural and magnetization characterization we found that the increase of T_C is directly related to the Nb–B bond length. Studies at high quasi-hydrostatic pressure show that T_C decreases, by reducing $N(E_F)$; we assume that the Fermi level is displaced to a minimum in $N(E)$, according to theoretical studies. Finally, the critical magnetic fields were determined at low temperature, showing values of about 200 and 2200 Oe for H_{C1} and H_{C2} respectively.

Acknowledgments

We thank DGAPA-UNAM for financial support, and F Silvar for technical support.

References

[1] Nagamatsu J, Nakagawa N, Muranaka T, Zenitani Y and Akimitsu J 2001 *Nature* **410** 63
[2] Indenbom M V, Uspenskaya L S, Kulakov M P, Bdikin I K and Zver'kov S A 2001 *Pis. Zh. Eksp. Teor. Fiz.* **74** 304

[3] Shein I R and Ivanovskii A L 2002 *Phys. Solid State* **44** 1833
Shein I R *et al* 2003 *Phys. Solid State* **45** 1617
Ivanovskii A L 2003 *Phys. Solid State* **45** 1829
[4] Kortus J, Mazin I I, Belashchenko K D, Antropov V P and Boyer L L 2001 *Phys. Rev. Lett.* **86** 4656
[5] Gasparov V A, Sidorov N S, Zver'kova I L and Kulakov M P 2001 *JEPT Lett.* **73** 532
Kaczorowski D, Zaleski A J, Zogal O J and Klamut J 2001 *Preprint* cond-mat/0103571
[6] Ziegler W T and Young R A 1953 *Phys. Rev.* **90** 115
[7] Hulm J K and Matthias B T 1951 *Phys. Rev.* **82** 273
[8] Leyarovska L and Leyarovski E 1979 *J. Less-Common Met.* **67** 249
[9] Cooper A S, Corenzwit E, Longinotti L D, Matthias B T and Zachariasen W H 1970 *Proc. Natl Acad. Sci.* **67** 313
[10] Schirber J E, Overmyer D L, Morosin B, Venturini E L, Baughman R, Emin D, Klesnar H and Aselage T 1992 *Phys. Rev.* B **45** 10787
[11] Kotegawa H, Ishida K, Kitaoka Y, Muranaka T, Nakagawa N, Takagiwa H and Akimitsu J 2002 *Physica* C **378–381** 25
[12] Yamamoto A, Takao C, Masui T, Izumi M and Tajima S 2002 *Physica* C **383** 197
[13] Akimitsu J 2001 *Annual Mtg of Physical Society of Japan* vol 3, p 533
[14] Altomare A, Burla M C, Giacovazzo C, Guagliardi A, Moliterni A G G, Polidori G and Rizzi R 2001 *J. Appl. Crystallogr.* **34** 392
[15] Falconi R, Durán A and Escudero R 2001 *Phys. Rev.* B **65** 024505
[16] Muzzy L E, Avdeev M, Lawes G, Haas M K, Zandbergen H W, Ramirez A P, Jorgensen J D and Cava R J 2002 *Physica* C **382** 153
[17] Kiessling R 1947 *Acta Chem. Scand.* **1** 893
[18] Higashi I, Takahashi Y and Okada S 1986 *J. Less-Common Met.* **123** 277
[19] Klesnar H, Aselage T L, Morosin B and Kwei G H 1996 *J. Alloys Compounds* **241** 180
[20] Slusky J S, Rogado N, Regan K A, Hayward M A, Khalifah P, He T, Inumaru K, Loureiro S M, Haas M K, Zandbergen H W and Cava R J 2001 *Nature* **410** 343
[21] Prassides K, Iwasa Y, Ito T, Chi D H, Uehara K, Nishibori E, Takata M, Sakata M, Ohishi Y, Shimomura O, Muranaka T and Akimitsu J 2001 *Phys. Rev.* B **64** 012509
[22] Goncharov A F, Struzhkin V V, Gregoryanz E, Hu J, Hemley R J, Mao H K, Lapertot G, Bud'ko S L and Canfield P C 2001 *Phys. Rev.* B **64** 100509
[23] Schlachter S I, Fietz W H, Grube K and Goldacker W 2002 *Advances in Cryogenic Engineering, ICMC'01: Proc. Int. Cryogenic Materials Conf. (Madison, July 2002)* p 809
[24] Bordet P J, Mezouar M, Nuñez-Regueiro M, Monteverde M, Nuñez-Regueiro M D, Rogado N, Regan K A, Hayward M A, He T, Loureiro S M and Cava R J 2001 *Phys. Rev.* B **64** 172502
[25] Friedel J and Dénoyer F 1987 *C. R. Acad. Sci.* II **305** 171